Exploring and strengthening the potential of R-phycocyanin from Nori flakes as a food colourant

Luka Veličković, Ana Simović, Nikola Gligorijević, Aurélien Thureau, Milica Obradović, Tamara Vasovic, Georgios Sotiroudis, Maria Zoumpanioti, Annie Brûlet, Tanja Ćirković Veličković, et al.

Exploring and strengthening the potential of R-phycocyanin from Nori flakes as a food colourant

Luka Veličković[a], Ana Simović[a], Nikola Gligorijević[b], Aurélien Thureau[c], Milica Obradović[a], Tamara Vasovic[a], Georgios Sotiroudis[d], Maria Zoumpanioti[d], Annie Brûlet[e], Tanja Ćirković Veličković[a,f,g,h], Sophie Combet[e], Milan Nikolić[a], Simeon Minić[a*]

[a] *University of Belgrade - Faculty of Chemistry, Center of Excellence for Molecular Food Sciences & Department of Biochemistry, Studentski trg 12–16, 11000 Belgrade, Serbia*

[b] *University of Belgrade - Institute of Chemistry, Technology, and Metallurgy, National Institute of the Republic of Serbia, Department of Chemistry, Studentski trg 12–16, 11000 Belgrade, Serbia*

[c] *SWING beamline, Synchrotron SOLEIL, Saint-Aubin BP 48, 91192 Gif-sur-Yvette, France*

[d] *National Hellenic Research Foundation (NHRF), Institute of Chemical Biology, 48 Vassileos Constantinou Ave., Athens 11635, Greece*

[e] *Université Paris-Saclay, Laboratoire Léon-Brillouin, UMR12 CEA-CNRS, CEA-Saclay, Gif-sur-Yvette CEDEX, France*

[f] *Centre for Food Chemistry and Technology, Ghent University Global Campus, Incheon, South Korea*

[g] *Department of Food Technology, Safety and Health, Faculty of Bioscience Engineering, Ghent University, Coupure Links 653, geb. A, B-9000 Ghent, Belgium*

[h] *Serbian Academy of Sciences and Arts, 11000 Belgrade, Serbia*

*Corresponding author:
Simeon Minic, PhD
University of Belgrade - Faculty of Chemistry, Center of Excellence for Molecular Food Sciences & Department of Biochemistry
Studentski trg 12-16, 11000 Belgrade, Serbia
E-mail: sminic@chem.bg.ac.rs

Abstract

This study aimed to purify, characterise and stabilise the natural food colourant, R-phycocyanin (R-PC), from the red algae *Porphyra* spp. (Nori). We purified R-PC from dried Nori flakes with a high purity ratio ($A_{618}/A_{280} \geq 3.4$) in native form (α-helix content 53%). SAXS measurements revealed that R-PC is trimeric ($(\alpha\beta)_3$) in solution. The thermal denaturation of α-helix revealed one transition (T_m at 52 °C), while the pH stability study showed R-PC is stable in the pH range 4 to 8. The thermal treatment of R-PC at 60 °C has detrimental and irreversible effects on R-PC colour and antioxidant capacity (22 % of residual capacity). However, immobilisation of R-PC within calcium alginate beads completely preserves R-PC colour and mainly retains its antioxidant ability (78 % of residual capacity). Results give new insights into the stability of R-PC and preservation of its purple colour and bioactivity by encapsulation in calcium alginate beads.

Keywords: R-phycocyanin, Purification, Stability, SAXS, Immobilization, Calcium alginate.

Introduction

Alternative proteins have recently gained increasing attention due to substantial environmental and health impacts compared to meat consumption (Onwezen, Bouwman, Reinders, & Dagevos, 2021). Algae are a promising source of alternative proteins as they can meet health, nutritional, environmental and production needs (Diaz et al., 2022). Red macroalgae *Porphyra* spp., commonly known as Nori, is a rich source of proteins, vitamins, minerals and antioxidants and has been used as food for centuries in Asia, and its popularity has now spread to other parts of the world (Bito, Teng, & Watanabe, 2017; Simovic, Combet, Cirkovic Velickovic, Nikolic, & Minic, 2022). Consumed as dried Nori flakes, it is frequently used to prepare sushi, soup and cakes (Bito et al., 2017). The most abundant proteins in *Porphyra* spp. are the phycobiliproteins (PBPs) R-phycoerythrin (R-PE) and R-phycocyanin (R-PC), contributing to approximately 3 % of the dry mass of *Porphyra* spp. (Cao, Wang, Wang, & Xu, 2016). Considering that nearly one million tons of *Porphyra* are produced annually (Baweja, Kumar, Sahoo, & Levine, 2016), R-PC and R-PE have great potential to be used as alternatives to animal proteins. Besides R-PE and R-PC, *Porphyra* spp. also contains the third phycobiliprotein allophycocyanin (APC), the minor protein of the PBP family (Liu et al., 1998). Compared to R-PE, which has been thoroughly studied, much less is known about the properties of R-PC of *Porphyra* spp.

R-phycocyanin is a strongly fluorescent and water-soluble molecule whose primary function is to transfer excitation energy to reaction centres during photosynthesis (Glazer & Hixson, 1975; Jiang, Zhang, Chang, & Liang, 2001). The intensive purple colour of R-PC arises from its covalently attached (*via* thioether bond) linear tetrapyrrole chromophores, phycoerythrobilin (PEB) and phycocyanobilin (PCB). It is composed of two subunit types forming a trimer $(\alpha\beta)_3$ or hexamer $(\alpha\beta)_6$, with α subunits of 18–20 kDa and β subunits of 19–21 kDa (Jian et al., 2001). One PCB chromophore is bound to both α and β subunits, while one PEB chromophore is only attached to β subunits.

R-phycocyanin has potential bioactive properties due to the potent antioxidant, immunomodulatory and anticancer activities of covalently bound tetrapyrrole chromophores (Guo et al., 2022; Rashed, Hammad, Eldakak, Khalil, & Osman, 2023). The health benefits of R-PC, its brilliant fluorescence, vivid colour, and the need to replace synthetic dyes give R-PC great potential for food fortification and colouring. Nori seaweed represents an essential source of R-PC as natural food colourant because it can be cultivated in vast amounts, as described above. Hence, tons of R-PC could be produced annually to colour different foods and beverages. However, in this perspective, R-PC's limited stability is the major obstacle. Indeed, generally, PBPs have moderate pH stability (Munier et al., 2014; Yan et al., 2010), and their thermal stability is low: an increase in temperature above 40 ^{o}C induces a substantial decrease in protein stability and colour intensity (Faieta, Neri, Sacchetti, Di Michele, & Pittia, 2020; Munier et al., 2014; Simovic et al., 2022).

Therefore, developing R-PC as a natural food colourant and alternative protein requires a deeper understanding of its structural and functional properties and improved stability. One promising approach for stabilising R-PC and other PBPs could be encapsulation in solid food matrices, which may decrease the mobility of protein molecules, making them more resistant towards temperature and oxidation processes (Maghraby, El-Shabasy, Ibrahim, & Azzazy, 2023). In this context, alginate immobilisation is a valuable strategy since it is widely used in biotechnology and bioprocessing for the entrapment of living cells, proteins, and other biological molecules (Andersen, Auk-Emblem, & Dornish, 2015). Alginate is a natural polysaccharide derived from brown seaweed and has unique physical and chemical properties that make it ideal for immobilisation. The process involves the formation of calcium-alginate beads, which can be easily manipulated and controlled in terms of size, shape and mechanical stability (Segale, Giovannelli, Mannina, & Pattarino, 2016).

In the present study, we aim to purify, characterise and stabilise the purple protein R-PC from dried Nori flakes for the first time. We used precipitation and chromatography techniques to obtain pure protein. Optical spectroscopy and SAXS measurements conclude that purified protein is a typical R-PC, with α-helix as the dominant secondary structure and trimeric oligomerisation state in solution. We determined the sequence of R-PC from Nori flakes by mass spectrometry and compared it with phycocyanins from other sources. Further, we employed absorption and far-UV CD spectroscopy to study the effects of temperature and pH on protein stability. Ultimately, we tested if R-PC immobilisation within calcium alginate beads could improve protein thermal stability and preserve its antioxidant capacity.

2. Materials and Methods

2.1 Materials

Dried Nori flakes (*Porphyra* spp.) were purchased from Fujian Friday Trading Co. LTD (China). Hydroxyapatite (HA) and diethyl aminoethyl (DEAE) Sepharose resins were bought from BioRad (CA, USA) and Sigma (MO, USA), respectively. Sodium alginate used for immobilisation was of food grade, purchased from Health Leads (France). All other chemicals were of analytical reagent grade.

2.2 R-PC isolation and purification

R-Phycocyanin was purified according to the previously published procedures with modifications (Boussiba & Richmond, 1979; Simovic et al., 2022; Wang et al., 2014). Nori seaweed leaves were frozen with liquid nitrogen and then pulverised using a mortar and pestle. The powdered sample was then suspended in 20 mM phosphate buffer pH 7.0 (1 g of powdered sample *per* 20 mL of buffer). Extraction of phycobiliproteins was performed overnight at 4 °C with constant stirring.

The resulting slurry was centrifuged at 6000 x g for 30 min at 6 °C. Proteins in the supernatant were precipitated with ammonium sulfate (65 % final concentration). The pellet was dissolved in 2.5 mM phosphate buffer pH 7.0 and was dialysed against the same buffer.

The dialysed solution was applied to the CHT ceramic hydroxyapatite (HA) column, previously equilibrated with the same buffer. Non-bound proteins (mainly R-PE) were washed away with the equilibration buffer, while fractions enriched with R-PC were obtained by stepwise elution protocol employing increasing concentrations of sodium phosphate salt (pH 7.0; **Fig. 1A**). R-PC containing fraction was applied onto the DEAE Sepharose CL-6B column, previously equilibrated with 20 mM phosphate buffer pH 7.0. Unbound proteins were flushed with an equilibration buffer. Bound proteins were eluted stepwise, increasing the ionic strength of NaCl from 0.05 to 0.2 M (**Fig. 1B**). The R-PC-rich fractions were pulled, desalted and concentrated. Purified R-PC was stored in 40 % (v/v) glycerol solution at -20 °C. We analysed the obtained fractions by UV-Visible absorption spectroscopy (**Section 2.3**) and SDS-PAGE under reducing conditions. Fluorescent PBP bands were first visualised under UV light, followed by staining with Coomassie Brilliant Blue R-250.

2.3 Determination of R-PC amino acid sequence by mass spectrometry

Purified R-PC was digested by trypsin, and obtained peptides were analysed by nano Liquid Chromatography-electron spray ionisation coupled to tandem mass spectrometry (nLC-ESI-MS/MS). The protein identification was performed using PEAKS Suite X (Bioinformatics Solutions Inc., Canada) software. Experimental details and mass spectrometry data analysis are given in Supplementary Material 1.

2.4 UV-Visible absorbance measurements

UV-Visible absorption spectra were recorded on a NanoDrop 2000c spectrophotometer (Thermo Scientific, USA) in a 1 cm pathlength quartz cell. The spectra were collected in the 250–750 nm range at room temperature. R-PC concentration was determined using the following equation (Nikolic, Minic, Macvanin, Stanic-Vucinic, & Velickovic, 2020):

$$R-PC\ \left(\frac{mg}{mL}\right) = 0.154(A_{618} - A_{730}) \qquad (1)$$

The effects of temperature and pH on visible absorption spectra of R-PC were studied using a UV-1800 Shimadzu spectrophotometer (Japan). Temperature measurements were performed using a Peltier element previously described (Simovic et al., 2022), and experimental details are given in Supplementary Material 1.

The pH dependence of R-PC absorption spectra was studied using the same measurement parameters described above for the thermal stability study. R-PC was incubated in the different

buffers (50 mM phosphate, citrate, Tris and glycine) in the pH range of 2–12 for 30 minutes, followed by the acquisition of absorption spectra at room temperature.

2.5 Fluorescence measurements

Fluorescence spectra of 1.8 μg/mL of R-PC at pH 7.0 were recorded with a FluoroMax®-4 spectrofluorometer (HORIBA Scientific, Japan) under thermostable conditions (25 °C), using 5 nm excitation and 5 nm emission slit widths. The PEB chromophore was excited at 488 and 590 nm, and the emission spectra were recorded between 520 and 610 nm. Excitation of PCB chromophore was performed at 590 nm, while the emission was measured in the range 610–680 nm.

The spectrofluorimetric oxygen radical absorbance capacity (ORAC) assay was performed according to Ou et al. (Ou, Hampsch-Woodill, & Prior, 2001). Stock solutions of fluorescein (5 μM) as the substrate and 2,2′-azobis(2-amidinopropane) dihydrochloride (AAPH, 300 mM) as the free radical generator were made in 75 mM sodium phosphate buffer, pH 7.4. The assay was performed: 50 μL of 100 μg/mL R-PC solution (obtained as described in **section 2.7**) was mixed with 1680 μL of buffer (75 mM phosphate, pH 7.4) and 20 μL of fluorescein solution. The reaction was initiated by the addition of 250 μL of AAPH solution. Fluorescence was measured at the excitation wavelength of 485 nm and an emission wavelength of 511 nm at 37 °C. Bandwidths of slits were set to 2 nm. The fluorescence was recorded every 20 seconds for 30 min. Measurements of blank samples (**section 2.7**) were performed in the same conditions. The blank sample's area under the curve (AUC) was subtracted from the corresponding AUC of R-PC-containing samples, and results were expressed as AUC per mg of R-PC. Measurements were performed at least in duplicate, and results were presented as mean ± standard deviation. For the evaluation of antioxidant capacity, an analysis of variance (ANOVA) of data was performed and means comparisons were made using the Tukey test.

2.6 CD spectroscopy measurements

CD measurements were carried out on a Jasco J-815 spectropolarimeter (Jasco, Japan) under constant nitrogen flow. All spectra were recorded at 25 °C. For the near-UV and visible region (250–750 nm), the concentration and pH of R-PC were set to 0.3 g/L and 7.0, respectively. Scan speed and the number of accumulations were set to 200 nm/min and two, respectively. A cell with an optical pathlength of 1 cm was used.

Far-UV CD spectra of 100 μg/mL R-PC have been recorded in the range 190–260 nm at a scan speed of 50 nm/min, using a cell with an optical pathlength of 1 mm and with an accumulation of three scans. Spectra were measured in different buffers in the pH range of 2–12 (**section 2.3**). The CD data analysis is given in Supplementary Material 1.

Thermal unfolding R-PC was performed as previously described (Simovic et al., 2022), and experimental details and data analysis are given in Supplementary Material 1.

2.7 SAXS experiments and analysis

SAXS spectra were obtained on the SWING beamline at the French synchrotron facility SOLEIL (St-Aubin, France) (Thureau, Roblin, & Pérez, 2021) using a wavelength of λ = 0.764 Å and a sample-to-detector distance of 3 m. The achievable q-range was 0.0033 to 0.531 $Å^{-1}$, where $q = \frac{4\pi}{\lambda} sin\vartheta$ is the modulus of the momentum transfer, and 2θ *is* the scattering angle. 40 µL of 5 mg/mL of R-PC at pH 5.7 (20 mM MES containing 150 mM NaCl) and buffer were injected into a 1.5 mm outside diameter quartz capillary thermalised at 15 °C.

The SAXS data analysis is given in Supplementary Material 1.

2.8 Immobilisation of R-PC in sodium alginate

The R-PC immobilisation in alginate hydrogel beads according to a previously published procedure (Zhang, Zhang, Zou, & McClements, 2016) with modifications. A solution of R-PC (4 mg/mL) was prepared in 25 mM acetate buffer at pH 5. Subsequently, this solution was mixed with a 2 % aqueous solution of sodium alginate in a volume ratio of 1:1. The resulting mixture was then droplet-wise deposited into a 2 % calcium chloride solution of 50 mM acetate buffer at pH 5. The formed beads were stored at 4 °C overnight. The beads containing immobilised proteins were thoroughly washed several times with 50 mM acetate buffer pH 5. The beads were then transferred into a microtube and subjected to thermal treatment at 60 °C for 10 minutes. Beads were dissolved using 100 mM Tris-citrate buffer pH 7.3. Obtained solutions were subjected to an ORAC test (**section 2.5**) to assess the effects of immobilisation and thermal treatment on the antioxidative capacity of R-PC. The dissolved beads without R-PC served as a blank in the ORAC assay. The control experiment comprises heating 2 mg/mL R-PC in solution (non-immobilised) at the same conditions as those used for the thermal treatment of the R-PC containing alginate beads.

3. Results

3.1 Purification of R-PC from Nori seaweed

We combined precipitation and chromatographic techniques to purify R-PC from Nori flakes. Phycobiliproteins from Nori seaweed exhibit the characteristic absorption peaks: R-PE (peaks at 498 and 560 nm, and shoulder at 545 nm), R-PC (peaks at 550–560 and 618 nm) and APC (peak at 652 nm with a shoulder at 620 nm) (Glazer et al., 1975; Simovic et al., 2022). Obtained raw extract had a strong absorption in the region from 250 to 450 nm due to the presence of various pigments (**Fig. 1C**). Precipitation with ammonium sulphate (65 %) increased the purity ratio (A_{618}/A_{280}) from 0.31

to 0.61 (**Fig. 1C**) by separating most of the non-protein related pigments absorbed in the region 250–450 nm. Different PBPs were not distinguished in this step since ammonium sulphate induces non-selective precipitation of all PBPs presented in the extract (**Fig. 1C**). Separation of R-phycocyanin from R-PE was achieved by applying HA chromatography (**Fig. 1A**). Most R-PE is eluted by equilibration buffer. At the same time, R-PC exhibits much stronger binding to the HA column and 100 mM phosphate is required for its elution. This chromatography step substantially increases A_{618}/A_{560} ratio (1.10) compared to the sample before chromatography (0.67). Although this step removed a significant amount of R-PE, the ratio of A_{618}/A_{280} was still low (1.32), suggesting the presence of other proteins in the R-PC enriched fraction. The same findings are observed by SDS-PAGE after the fluorescence visualisation of PBPs and CBB staining (**Fig. 1D**). Hence, anion-exchange chromatography on DEAE-Sepharose was employed to purify R-PC further. The chromatogram displayed two peaks, with the R-PC fraction eluting ionic strength of 150 mM NaCl. The fraction that was eluted with 200 mM NaCl corresponded to allophycocyanin and R-PE (high binding fraction).

Combining HA and ion-exchange chromatography resulted in the preparation of R-PC with a purity index of A_{618}/A_{280}, around 3.4. The absence of a shoulder at 498 nm in absorption spectra (Simovic et al., 2022), which indicates the complete removal of R-PE (**Fig. 1C**) and the presence of solely two characteristic bands in the electrophoretic profile (**Fig. 1D**) served as confirmation that R-PC of the high purity is obtained. The two observed bands at ~18 and 20 kDa arise from α and β subunits of R-PC. Interestingly, visualisation of SDS-PAGE gel by UV lamp revealed that β subunits exhibit much stronger fluorescence than α subunits. This result could be ascribed to the higher quantum yield of PEB chromophore (Grabowski & Gantt, 1978; Saraswat et al., 2011), exclusively bound to the R-PC β subunits, compared to the PCB chromophore, which is attached to both α and β subunits.

3.2 Spectroscopic and structural characterisation of purified R-phycocyanin

The purified R-PC was digested by trypsin, and we analysed obtained peptides by tandem mass spectrometry. Based on this analysis (**Supplementary Material 2**), the R-PC sequence of both subunits (α and β) was determined (**Fig. 2A**). Furthermore, we identified the binding sites for tetrapyrrole chromophores: α subunit binds one chromophore *via* Cys84, while two chromophores are attached to β subunit by Cys82 and Cys153 (**Fig. 2A**). Considering the same molecular mass of PCB and PEB, we could not make a distinction between them in MS spectra, but only the position of Cys residue involved in chromophore binding. However, based on the previously published crystal structure of R-PC from *Polysiphonia urceolata* (Jiang et al., 2001), we were able to assign PCB binding to Cys84 and Cys82 of α and β subunits, respectively, while PEB chromophore is bound to

the Cys153 of β subunits. BLAST analysis revealed the high sequence identity (around 90% or higher) between obtained R-PC from *Porphyra* spp. and other phycocyanins belonging to the different classes of *Rhodophyta* division (**Tables S1 and S2**). We also detected about 70% of sequence homology with the C-phycocyanin from cyanobacteria *Spirulina* with the identical position of Cys residues involved in the chromophore binding sites (Minic et al., 2016).

As previously described, the VIS absorption spectrum of purified R-PC exhibited two characteristic peaks at 552 and 618 nm, originating from PEB and PCB chromophores, respectively (**Fig. 1C**). The presence of two PCB chromophores per αβ heterodimer of R-PC gives higher absorption of the peak at 618 nm compared to the peak intensity at 552 nm, because only one PEB chromophore is bound to β subunit. Excitation of PEB and PCB chromophores in R-PC at 488 and 590 nm gives two intensive emission peaks at 580 and 640 nm, respectively (**Fig. 2B**). In accordance with the absorption spectra, the higher content of PCB compared to PEB chromophores in R-PC (2 *vs* 1, respectively) gives stronger emission at 640 nm compared to 580 nm. PEB and PCB chromophores are in the asymmetric environment within the R-PC structure, which induces strong signals in the near-UV/visible CD spectrum of this protein. In the visible region, two peaks appear that originate from PEB (540 nm) and PCB (634 nm) chromophores (**Fig. 2C**). We also observed two peaks at 306 and 341 nm, arising from a higher excitation state of the PEB and PCB chromophores, respectively (**Fig. 2C**) (Glazer et al., 1975). Interestingly, we observed the differences in the shape and the position of peaks in the CD spectra of PEB and PCB chromophores (10–20 nm) compared to absorption spectra, especially in terms that the relative intensity of PEB band is stronger in CD compared to the absorption spectra. This finding indicates the strong interactions of tetrapyrrole chromophores between different subunits within R-PC oligomers (Glazer et al., 1975).

Far-UV CD spectra were recorded to characterise the secondary structure of purified R-PC. As shown in **Fig. 2D**, the far-UV CD spectra of R-PC have negative ellipticity between 202 and 240 nm, with minima at 209 and 222 nm and also show a positive ellipticity at 192 nm, which corresponds to the signals of α-helical proteins. Indeed, α-helix is the main secondary structure in R-PC (53 %).

SAXS measurements were performed to determine the R-PC shape and oligomerisation state in solution at pH 5.7. A well-defined plateau characterises the SAXS profile of R-PC at $Q < 0.01$ $Å^{-1}$ (**Fig. 2E**), confirming the absence of aggregates in the purified protein. We also observed the large shoulder at 0.1 $Å^{-1}$, arising from the central hole in the R-PC structure (**Fig. 2E**). Indeed, we demonstrated by CRYSOL software that our experimental SAXS curve fits well with the theoretical curve of the crystal structure of trimeric R-PC (**Figs. 2E and 2F**) from *Polysiphonia urceolata* (Chang et al., 1996), which resembles the shape of the hollow cylinder. Indeed, SAXS intensities are well fitted to a hollow cylinder analytical model (**Fig. S1**), enabling us to determine the R-PC dimensions (**Fig. 2F**). We also performed the *ab initio* modelling by GASBOR software (**Figs. 2G** and **2H**)

without making any assumption of R-PC structure and obtained a model that closely resembles the R-PC crystal structure and hollow cylinder analytical model (**Fig. 2F**). Radii of gyration value (R_g = 39.3 Å), obtained from Guinier plots, is in very good agreement with the previously determined R_g values for trimeric phycocyanin (**Saxena, 1988**).

3.3 R-phycocyanin thermal stability

The thermal stability of the R-PC has been determined using CD and UV/VIS absorption spectroscopy. CD spectroscopy has allowed us to follow the temperature variation of the ellipticity at 222 nm, indicating the loss of the α-helical structure. The resulting melting curve, shown in **Fig. 3A**, exhibits one steep transition with a melting temperature of 52 °C (325 K) and an apparent unfolding enthalpy of 385.5 kJ/mol.

In an alternative approach, we evaluate R-PC's thermal stability by studying the absorption spectra changes. The results, shown in **Fig. 3B**, indicate that up to 40 °C, no significant differences in the spectral characteristics of the protein are observed. However, as the temperature is increased further (above 45 °C), a substantial decrease in absorption intensity is observed in the region between 500 and 700 nm, followed at 55 °C and above, by the disappearance of the characteristic bands associated with PCB and PEB. Additionally, at temperatures above 50 °C, a substantial increase of absorbances at lower wavelengths (below 500 nm) indicates the aggregation of unfolded proteins. These findings suggest that R-phycocyanin undergoes significant structural changes at higher temperatures, leading to the loss of its characteristic spectral features. Reducing the temperature to 20 °C did not lead to the recovery of distinct absorption bands, indicating an irreversible protein denaturation (**Fig. 4A**).

3.4 R-phycocyanin pH stability

The pH stability of R-PC was assessed using UV/VIS absorption spectrometry. Spectral analysis of R-PC in the pH range 4–8 revealed well-defined absorption maxima. A noteworthy absorbance increase at 552 nm was observed for pH between 4 and 5. In contrast, the peak at 618 nm displayed similar absorbance intensity throughout the pH range 4–8 (**Fig. 3C**), indicating that moderate acidic conditions do not induce conformational changes in the vicinity of the PCB chromophore. Further increase or decrease of pH (9 and 3, respectively) triggered a significant reduction in the absorption intensities of both PEB and PCB chromophores, but without pronounced changes in the peak shapes. In extreme pH conditions (pH 2 and pH 10–12), both spectral bands of R-PC were substantially disturbed, indicating protein unfolding (**Fig. 3C**). At pH 2, a significant red shift in the spectrum occurs, suggesting the protonation of pyrrole rings within tetrapyrrole chromophores (Dietzek et al., 2004), while, at alkaline conditions, a blue shift in the R-PC spectrum indicates chromophores oxidation (Minic et al., 2018).

We examined the effects of pH on R-PC's secondary structures by far-UV CD spectroscopy (**Fig. 3D**). No significant change in the far-UV CD spectra shape was observed for pH values ranging from 3 to 9. Although at pH 3 and 9, the α-helical bands at 209 and 222 nm are still pronounced, a significant decrease in ellipticity (absolute values) is observed at these pH values (**Fig. 3D**), confirming the reduction in R-PC α-helical content. Furthermore, at both low acidic conditions (pH 2) and high alkaline conditions (pH above 9), we note the absence of the α-helix characteristic bands (**Fig. 3D**), suggesting a complete denaturation of the protein.

3.5 Thermal stability of R-phycocyanin immobilised in calcium alginate beads

We immobilised R-PC in calcium alginate beads, and obtained product was subjected to thermal treatment at 60 °C for 10 minutes. Our results demonstrate that the colour of R-PC immobilised in alginate beads does not change upon heating (**Fig. 4B**). On the other hand, as described above, heating of R-PC induces the detrimental loss of the protein colour (**Fig. 4A**). Therefore, immobilised R-PC exhibit greater thermal stability (**Fig. 4B**) compared to a protein that was not immobilised (**Fig 4A**). Furthermore, the absorption spectrum of the R-PC extracted from the calcium alginate matrix after thermal treatment showed no significant change, except a small increase in absorbance at wavelengths below 500 nm, which indicates a slight protein aggregation within alginate beads upon thermal treatment. Therefore, our findings provide strong evidence of the substantial thermal stabilisation of protein in the calcium alginate matrix.

We also employed an ORAC assay to test the effects of immobilisation and heating on the antioxidative capacity of R-PC. We did not observe any significant changes in the ORAC values between R-PC and immobilised R-PC protein before thermal treatment (**Fig. 5**). Heating R-PC has detrimental effects on the protein's antioxidant activity (**Fig. 5**). On the other hand, heating the immobilised R-PC preserved the antioxidant action in comparison to the heating R-PC in solution. However, the heat treatment decreased for ~20 % the antioxidant activity of immobilised R-PC compared to unheated immobilisate (**Fig. 5**), indicating that the immobilisation approach could not preserve the antioxidant capacity of R-PC upon heating completely.

4. Discussion

In this study, we purified and characterised the R-phycocyanin (R-PC) from dried Nori flakes. Further, we tested the stability of purified, food-derived R-PC using the combination of several experimental approaches. We observed the low-temperature stability of R-PC since a moderate thermal treatment induces irreversible loss of protein colour and antioxidant capacity. On the other hand, protein immobilisation inside alginate beads significantly improves R-PC thermal stability.

In the cells of algae, R-phycocyanin and homologous PBPs, like R-PE and APC, form large photosynthetic complexes called phycobilisomes (Saluri, Kaldmäe, & Tuvikene, 2019). Therefore, an important obstacle in R-PC purification is removing the other PBPs, especially R-PE, the most abundant protein in *Porphyra*. We tackled this challenge with a combination of HA and IEC chromatography. HA chromatography removed the majority of R-PE, while IEC separated R-PC from other proteins, including APC. The achieved R-PC purity ratio of 3.4 (A_{618}/A_{280}) was significantly higher than the purity of R-PC ($A_{618}/A_{280} < 3.0$) isolated from red macroalgae *Polysiphonia urceolata* (Wang et al., 2014). However, the commonly accepted criterion for the analytical grade purity of C-phycocyanin (C-PC) is 4 (Nikolic et al., 2020). C-PC and R-PC have three and two PCB chromophores, respectively. Hence, obtained R-PC purity between 3 and 4 could not be ascribed to impurities but to a lower number of PCB chromophores bounds compared to C-PC, which induces a lower A618/A280 ratio. Additionally, SDS-PAGE justified the R-PC purity and its heteromeric structure with two bands arising from α and β subunits. The heteromeric structure of purified R-PC has also been confirmed by mass spectrometry (MS). Moreover, we utilised MS to determine the sequence of R-PC from Nori flakes, and high sequence homology with phycocyanins from different classes of red algae and cyanobacteria has been detected.

Overall, we successfully optimised a protocol for producing high-purity vibrant purple-coloured R-PC. Although, to the best of our knowledge, there is no analysis on the costs of R-PC extraction and purification, the purity grade of phycocyanins, in general, strongly influences its commercial value. For example, the prices of C-PC from *Spirulina* range from $0.35 to $135 per gram in the food and cosmetics industries and up to $4600 per gram for therapeutic and diagnostic applications (Zittelli, Lauceri, Faraloni, Benavides, & Torzillo, 2023). However, the commercialisation of R-PC and other phycocyanins faces challenges due to their chemical instability and the high costs and time-consuming nature of extraction and purification methods (Fernandes et al., 2023, Zittelli, Lauceri, Faraloni, Benavides, & Torzillo, 2023). Therefore, there is a pressing need to scale R-PC production for industrial purposes to enable its sustainable production and meet market demands, representing essential aspects for future studies.

Optical spectroscopy and SAXS curves show typical features of R-PC: well-defined absorption, CD bands in the near-UV-VIS region and intensive fluorescence detectable at low nM concentrations (Wang et al., 2014). The specific feature of R-PC is the presence of additional bands in absorption, fluorescence and CD spectra, arising from the PEB chromophore, not presented in the cyanobacterial phycocyanins (Yan et al., 2010). The different peak positions between near-UV-VIS CD and absorption spectra of R-PC indicate strong exciton-type interactions between tetrapyrrole chromophores, confirming the oligomeric structure of the protein (Glazer et al., 1975; Li et al., 2020). Additionally, the stronger intensity of the PEB band compared to the PCB band in CD spectra, which

is opposed to the intensity ratio of these two bands in absorption spectra, could be ascribed to the deviation of the PEB chromophore D ring from BC rings conjugate plane, as observed in the crystal structure of R-PC from *Polysiphonia urceolata* (Jiang et al., 2001; Pescitelli et al., 2003). In this regard, it was previously shown that dihedral angles within and between chromophores significantly contribute to the intensities in CD spectra (Berova, Di Bari, & Pescitelli, 2007). Such an effect could be especially relevant within oligomeric PBPs where chromophores of different subunits could interact with each other. Indeed, our SAXS experimental curve of R-PC in solution (pH 5.7), purified from Nori (*Porphyra*), fits well with the theoretical curve of R-PC crystal structure from *Polysiphonia urceolata* in trimeric oligomer state, indicating conservation of R-PC 3D structure between different classes of organisms. Indeed, this finding is in accordance with the above-stated high sequence homology between *Porphyra* R-PC and phycocyanin from other sources. We also elucidated the structure of R-PC by the *ab initio* approach and found very good agreement with the model obtained by crystallography (Jiang et al., 2001). However, we observed that R-PC from red algae and C-PC from cyanobacteria do not have the same propensity towards oligomerisation. According to Saxena (Saxena, 1988), C-PC from the cyanobacterium Synechocystis sp. has a hexameric structure at pH 5.7, whereas R-PC is in a trimeric state here. Moreover, our SAXS results (data not shown) demonstrated that C-PC from *Spirulina*, the most cultivated microalgae for food purposes, also has a hexameric form at pH 5.7. This difference indicates that the unique presence of PEB chromophore in R-PC, but not in C-PC, could provoke the subtle conformational changes that influence the oligomerisation trend.

The native structure of R-PC was preserved in dried Nori flakes, as confirmed by high α-helical content (>50 %). Although (to the best of our knowledge) no previous studies are focusing on the far-UV CD spectra of R-PC, our results are in good agreement with the obtained α-helical content for C-PC from *Spirulina* and other cyanobacteria (Chen, Liu, MacColl, & Berns, 1983; Chi et al., 2020; Edwards, Hauer, Stack, Eisele, & MacColl, 1997; Li, Gillilan, & Abbaspourrad, 2021). However, R-PC has a substantially lower amount of α-helixes in comparison to R-PE (>70 %) (Simovic et al., 2022), suggesting the presence of γ subunit is the main contributor to the higher percentage of α-helix in R-PE.

Temperature increase induced a steep reduction in α-helix ellipticity, showing a one-transition unfolding of R-PC at T_m ~52 °C. Although (to the best of our knowledge) there is no data about the thermal stability of R-PC, the studies conducted on phycocyanins from *Spirulina* and other cyanobacteria (C-PC) obtained similar thermodynamic data with the melting temperature of C-PC in the range of 50-60 °C (Chen et al., 1983; Faieta et al., 2020). On the other hand, our previous CD study demonstrated higher thermal stability of the R-PE from *Porphyra* spp. due to a more stable γ subunit, a unique feature of the R-PE oligomer (Simovic et al., 2022). Absorption measurements

revealed that the R-PC colour is unstable above 40 °C. At the same time, the thermal treatment at 55 ºC or above induces the complete and irreversible loss of R-PC-specific bands in the absorption spectra. Although previous studies also confirmed that R-PE colour from Nori flakes starts to diminish above 40 ºC (Simovic et al., 2022), the R-PE specific absorption peaks, especially the band arising from γ subunit, could be observed up to 75 ºC. Therefore, the presence of γ subunit is R-PE's key structural feature, making its structure substantially more stable than R-PC. In this context, the previous studies demonstrated that phycocyanin from *Spirulina*, with the same subunit composition as R-PC, also has unstable colour at higher temperatures with the onset of colour loss above 40 ºC (Chaiklahan, Chirasuwan, & Bunnag, 2012; Faieta et al., 2020).

The colour of R-PC exhibits good stability in the pH range of 4–8, previously shown for phycocyanin from *Spirulina* (Li et al., 2021; Yan et al., 2010). The secondary structures (α-helices) of R-PC are also well preserved in the same pH range, confirming that tetrapyrrole chromophores are good indicators of the conformational state of PBPs. R-PE from red macroalgae has a slightly wider pH stability range (Munier et al., 2014), which is in accordance with the higher thermal stability of R-PE. Shifting the pH to more acidic (pH 3) or alkaline conditions (pH 9) will induce loss in α-helical structure and colour intensity of R-PC. However, the main spectral feature of R-PC is still preserved, indicating the absence of complete protein denaturation. A similar observation was made on C-PC from *Spirulina*, which was not entirely unfolded at pH 3 and 9 (Li et al., 2021; Zhang, Cho, Dadmohammadi, Li, & Abbaspourrad, 2021). Moreover, in contrast to R-PC, the α-helical structure in C-PC is mostly preserved at pH 9 (Li et al., 2021). Still, C-PC becomes more flexible, and dissociation from hexamers/trimers to monomers was observed at pH 9 (Li et al., 2021). Increasing the pH above 10 or acidification to pH 2 entirely unfolds R-PC, while tetrapyrrole chromophores oxidation at high pH was also observed. Considering that moderate acidic conditions (pH 3–4) do not have detrimental effects on R-PC colour and most fruit juices display pH in this range (Reddy, Norris, Momeni, Waldo, & Ruby, 2016), R-PC have a promising potential for applications as a colouring agent for soft beverages, even if its properties can be improved.

Porphyra spp. proteins have a high essential amino acid index, representing a sustainable alternative to animal proteins (Rawiwan, Peng, Paramayuda, & Quek, 2022). Further, the added value of *Porphyra* spp., as the source of alternative proteins, is the high abundance of PBPs characterised by the vivid colours and strong bioactive properties (Venkatraman & Mehta, 2019). These specific properties of PBPs substantially strengthen the consumer acceptance of *Porphyra* spp. as an alternative source of proteins. However, preserving the PBPs' colour and bioactivities during the food treatment is a significant challenge for enhancing their application in the food industry. Alginate hydrogel beads represent a promising system for encapsulating, protecting, and delivering food proteins (Zhang et al., 2016). Our study unambiguously confirmed that encapsulation of R-PC into

alginate beads completely preserves the protein colour upon thermal treatment at 60 ºC. Moreover, the antioxidative capacity of encapsulated R-PC is maintained largely upon thermal treatment but not wholly, probably due to slight protein aggregation within alginate beads, which could mask R-PC antioxidant activity. On the other hand, heating of R-PC that was not immobilised induces detrimental loss of protein colour and antioxidative activity, followed by aggregation of unfolded R-PC subunits. Indeed, previous studies demonstrated the ability of alginate-encapsulated C-PC from Spirulina to preserve its antioxidant capacity upon thermal treatment (Qiao et al., 2022). Therefore, encapsulating R-PC or other temperature-sensitive, food-derived PBPs into alginate beads could be an excellent approach to preserve and modulate its techno-functional properties, such as colour, aggregation and antioxidant capacity. Furthermore, this approach could be a good strategy for controlling the release of bioactive PBPs in the gastrointestinal tract (GIT) (Qiao et al., 2022). Alginate immobilisation in the presence of calcium ions represents the non-covalent entrapment of the protein of choice by making a gel-like network that surrounds the protein, thus entrapping it within (Zhang et al., 2016). Factors like pH and mechanical treatment could significantly affect the system's stability in this context. By having R-PC non-covalently immobilised, easier protein leakage is expected. This could be a double-edged sword. While the risk of leakage limits conditions at which alginate: R-PC beads can be stored and prevents rigorous mechanical treatments, this could be beneficial during their potential consumption since during the mechanical eating process of chewing and different pH values of GIT could easily release bioactive R-PC. On the other hand, the utilisation of composite gels which combine alginate with other biopolymers, such as chitosan, gelatin, and various proteins, improves the physical and mechanical properties of the gel, enhancing encapsulation efficiency, resulting in better protection and controlled release of bioactive compounds (McClements, 2018; Ramdhan, Ching, Prakash, & Bhandari, 2020).

5. Conclusions

We successfully purified and characterised the R-PC from commercially dried Nori flakes. The purified protein exhibited optical and structural characteristics of typical R-PC in the oligomeric (trimeric) α-helical structure. R-PC has moderate pH stability while being more stable in acidic than in alkaline conditions. It also has relatively low-temperature stability, and an irreversible colour change and antioxidant capacity loss were observed upon thermal treatment at 60 ºC. However, immobilisation of the R-PC inside calcium alginate beads significantly improved protein thermal stability and preserved its antioxidant capacity and colour.

Our results suggest that R-PC has a promising potential for colouring soft beverages at slightly-acidic conditions. However, further studies are needed to further improve its pH stability. Encapsulating R-PC into solid matrices could be an excellent approach to preserve protein colour and

bioactivities upon thermal processing, strengthening its potential for food colouring and positioning it as an ideal alternative protein.

Credit authorship contribution statement

Luka Velickovic: Investigation, Conceptualisation, Formal analysis, Writing – original draft. **Ana Simovic:** Investigation**,** Conceptualisation, Formal analysis, Writing – review and editing. **Nikola Gligorijevic:** Investigation, Conceptualisation, Formal analysis, Writing – review and editing. **Aurélien Thureau:** Investigation, Formal analysis. **Milica Obradovic:** Investigation. **Tamara Vasovic** – Investigation, Formal analysis. **Georgios Sotiroudis:** Investigation, Writing – review and editing. **Maria Zoumpanioti:** Writing – review and editing. **Annie Brûlet**: Investigation, Formal analysis, Writing – review and editing. **Tanja Cirkovic Velickovic**: Writing – review and editing. **Sophie Combet:** Investigation, Formal analysis, Writing – review & editing. **Milan Nikolic:** Conceptualisation, Funding acquisition, Supervision, Writing – review and editing. **Simeon Minic:** Investigation**,** Conceptualisation, Formal analysis, Funding acquisition, Supervision, Writing – review and editing.

Declaration of Competing Interest

The authors declare that they have no known competing financial interests or personal relationships that could have appeared to influence the work reported in this paper.

Acknowledgement

We are grateful to the SOLEIL synchrotron for the XR beam time (project 20220590), as well as the staff of the SWING beamline for assistance. This work was supported by: 1) The Alliance of International Science Organizations, Project No. ANSO-CR-PP-2021-01 2) Ministry of Science, Technological Development and Innovation of Republic of Serbia, contract number: 451-03-47/2023-01/200168 and 3) a short-term FEBS fellowship to Simeon Minić.

Figure legends

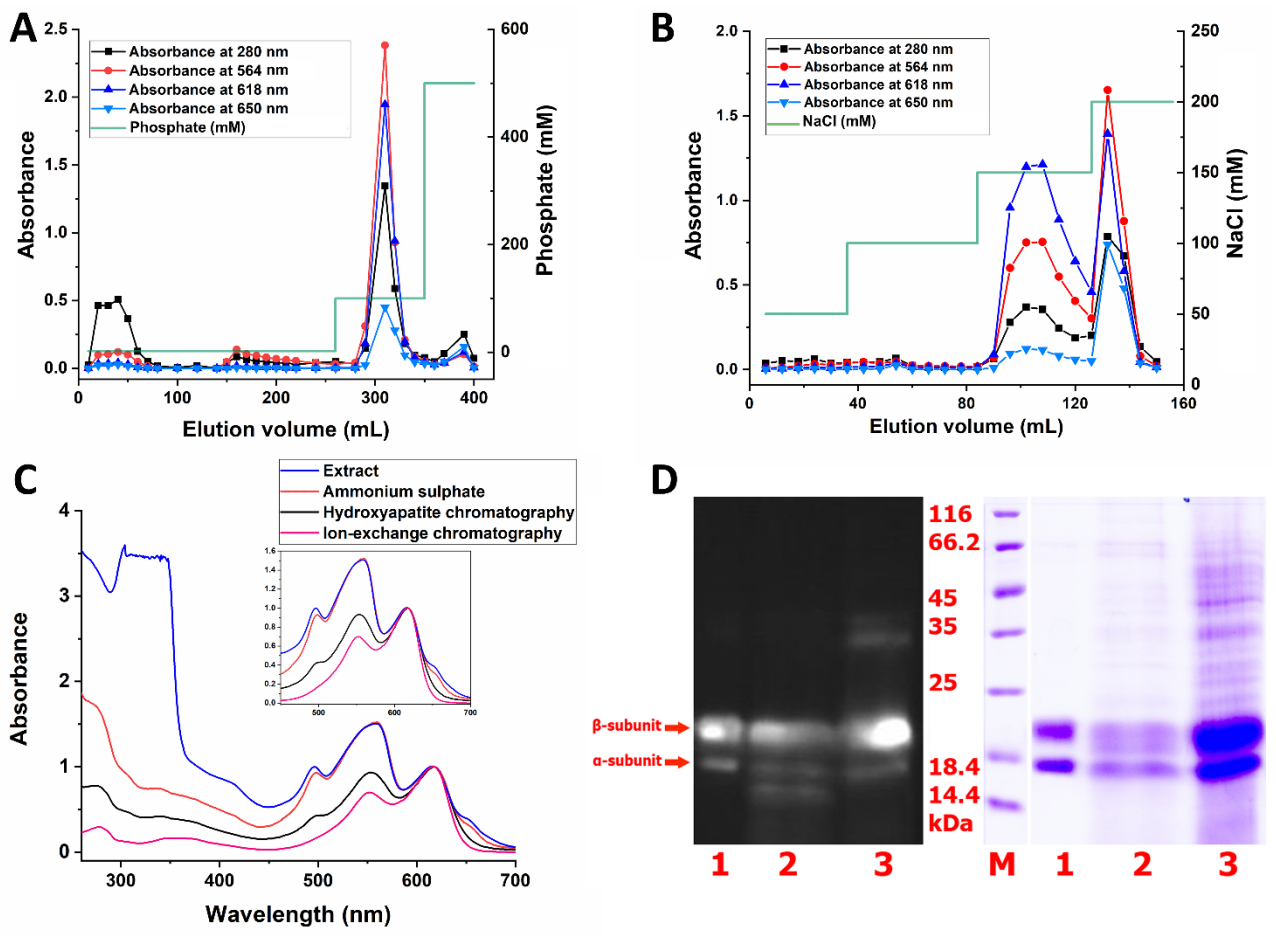

500

501 **Figure 1.** The chromatograms obtained after **(A)** hydroxyapatite and **(B)** ion-exchange
502 chromatography of R-PC; **(C)** Absorption spectra of R-PC after each purification step; **(D)** SDS-
503 PAGE electrophoresis under UV light (left) and after CBB staining (right) - lane 1: Purified RPC,
504 lane 2: hydroxyapatite eluate, lane 3: protein extract, M: molecular size markers.

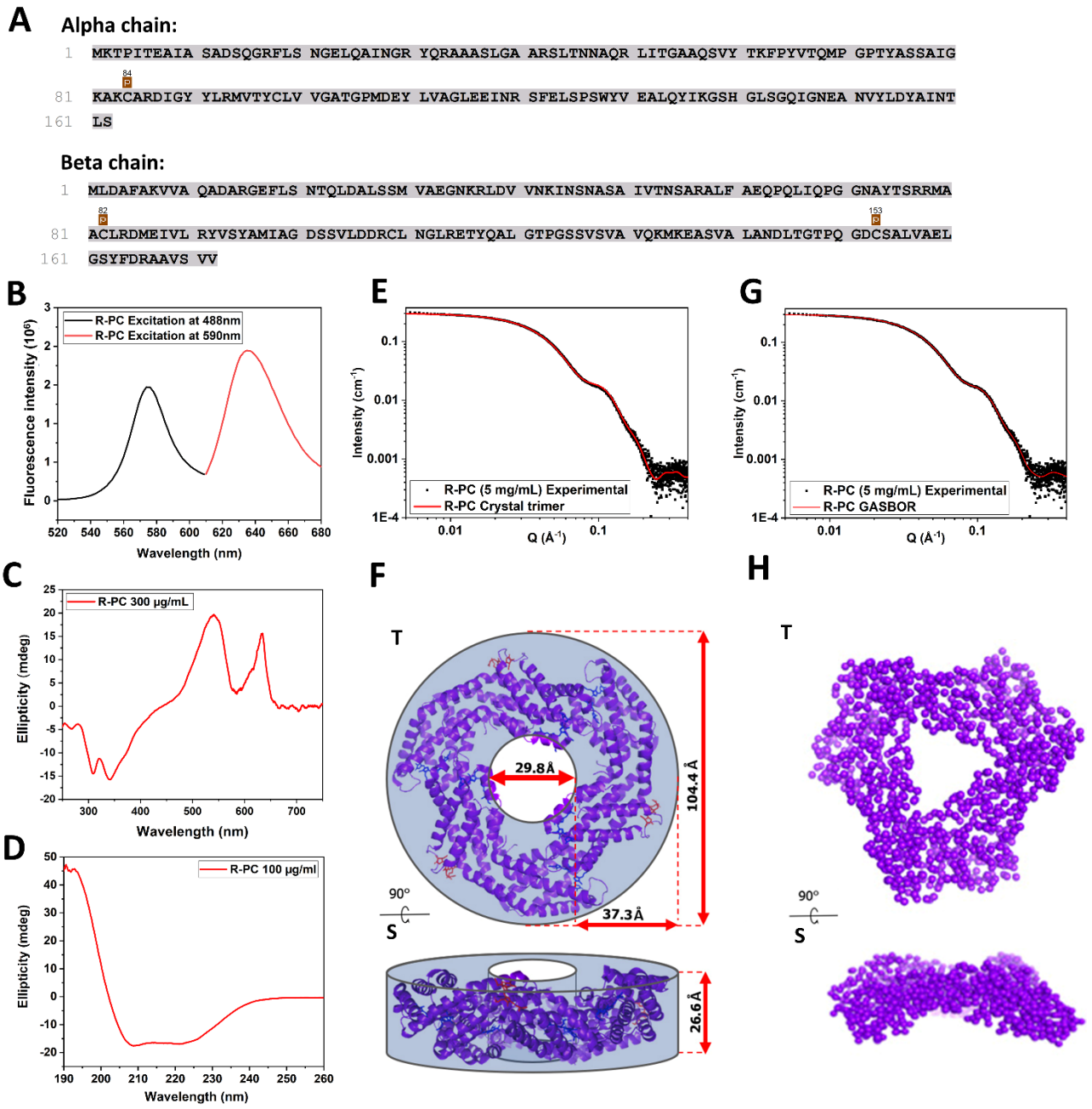

Figure 2. (**A**) Amino acid sequences of R-PC α and β subunits determined by mass spectrometry. P denotes the attachment site for PCB (Cys84 and Cys82 in α and β subunits, respectively) and PEB chromophores (Cys153 in β subunit); (**B**) Fluorescence emission spectra of purified R-phycocyanin (16 nM) after excitation at 488 nm (black line) and 590 nm (red line) at pH 7.0; (**C**) Near-UV/Visible and (**D**) far-UV CD spectra of R-PC (pH 7.0); (**E**) Comparison of the experimental SAXS curve of R-PC at pH 5.7 (dotted black line) with the theoretical curve (full red line) calculated from R-PC crystal structure (PDB:1F99) by CRYSOL software (ATSAS); (**F**) Ribbon model of the crystal structure of R-PC trimer superimposed with the hollow cylinder analytical model; Dimensions are obtained by the best fit to this model (**Table S3**). Obtained χ^2 value was 2.8; (**G**) Comparison of the same experimental SAXS curve with the curve obtained from *ab initio* modelling (full red line) using

GASBOR software (ATSAS). The obtained $\chi 2$ value was 1.5; (**H**) Ab initio envelope of the R-PC oligomer corresponding to the GASBOR model. T and S denote top and side views, respectively.

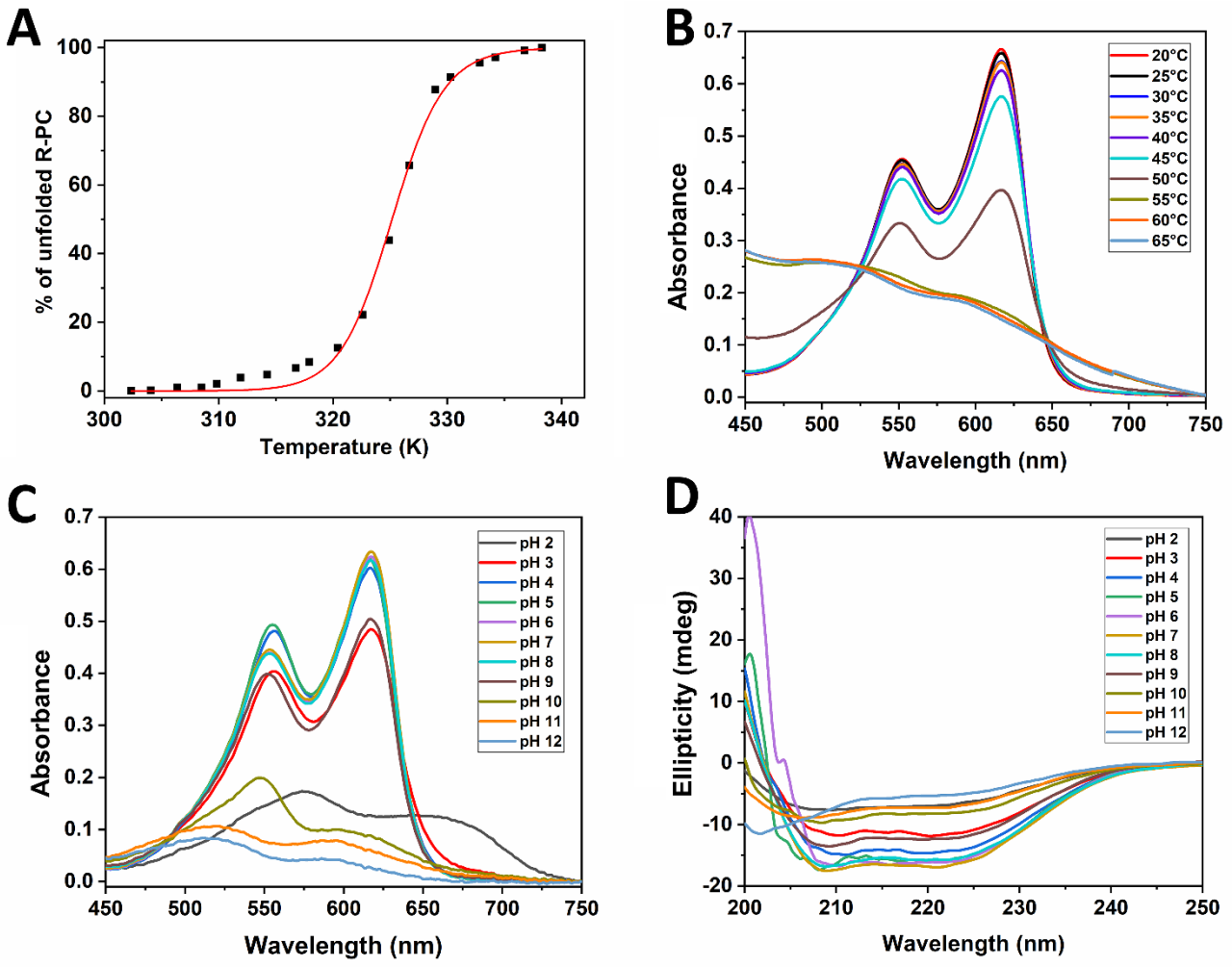

Figure 3. (**A**) 20 µg/mL (182 nM) R-PC thermal unfolding curve with the corresponding fit (full red line), obtained by measuring ellipticity at 222 nm and pH 7.0; (**B**) The effects of temperature on visible absorption spectra of 100 µg/mL (0.9 µM) R-PC at pH 7.0 (optical pathlength 1 cm); (**C**) The effects of pH on visible absorption spectra of 100 µg/mL R-PC at 25 °C; (**D**) The effects of pH on far-UV CD spectra of 100 µg/mL R-PC at 25 °C.

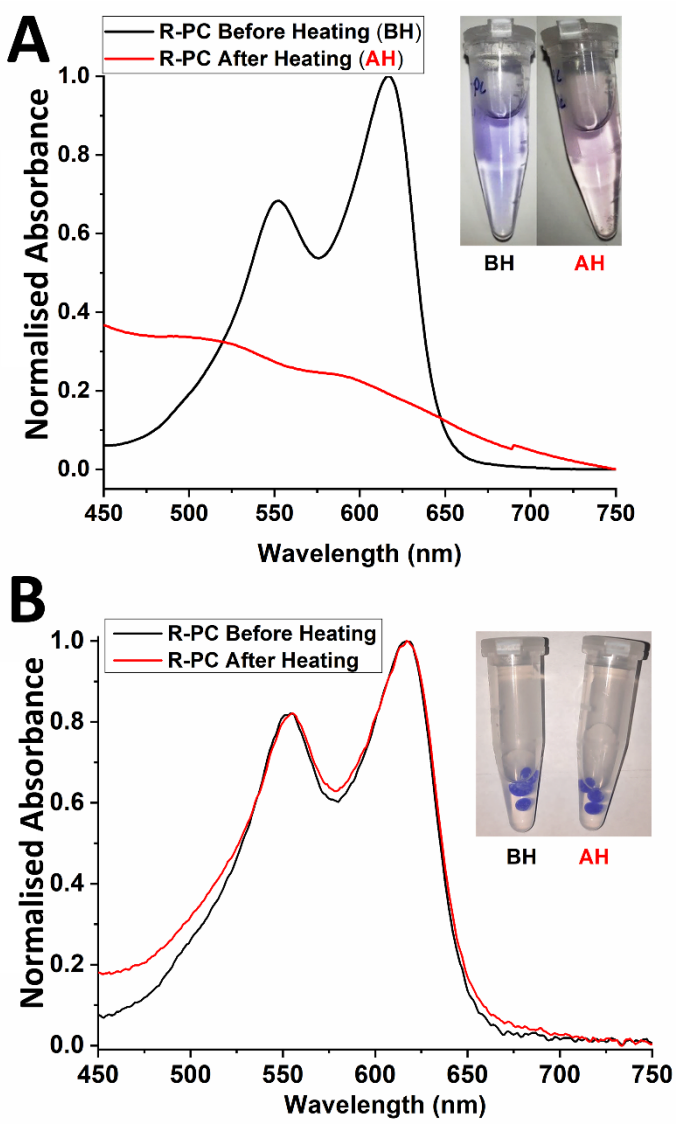

524

525 **Figure 4.** Absorption spectra of (**A**) R-PC without immobilisation and (**B**) R-PC extracted from
526 calcium alginate beads before and after heating at 60 °C for 10 min; Insets show pictures of (**A**) R-
527 PC without immobilisation and (**B**) immobilised R-PC before (BH) and after (AH) heating.

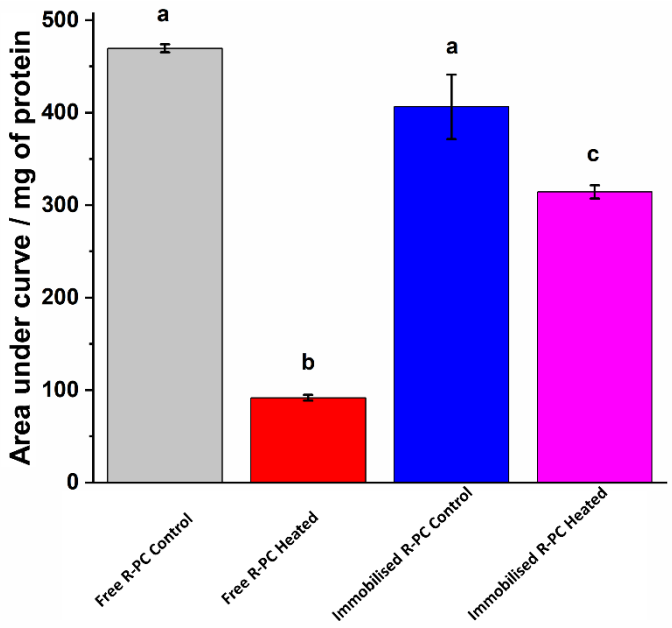

Figure 5. Histogram comparing antioxidative activity (ORAC assay) of R-PC without immobilisation (free R-PC) and R-PC immobilised in calcium alginate beads before and after heating at 60 °C. The data marked by different letters are significantly different ($p<0.05$).

References

Andersen, T., Auk-Emblem, P., & Dornish, M. (2015). 3D Cell Culture in Alginate Hydrogels. *Microarrays (Basel), 4*(2), 133–161. https://doi.org/10.3390/microarrays4020133

Baweja, P., Kumar, S., Sahoo, D., & Levine, I. (2016). Biology of Seaweeds. In J. Fleurence & I. Levine (Eds.), *Seaweed in Health and Disease Prevention* (pp. 41–106). Academic Press.

Berova, N., Di Bari, L., & Pescitelli, G. (2007). Application of electronic circular dichroism in configurational and conformational analysis of organic compounds. *Chemical Society Reviews, 36*(6), 914–931. https://doi.org/10.1039/b515476f

Bito, T., Teng, F., & Watanabe, F. (2017). Bioactive Compounds of Edible Purple Laver Porphyra sp. (Nori). *Journal of Agricultural and Food Chemistry, 65*(49), 10685–10692. https://doi.org/10.1021/acs.jafc.7b04688

Boussiba, S., & Richmond, A. E. (1979). Isolation and Characterisation of Phycocyanins from the Blue-Green Alga Spirulina platensis. *Archives of Microbiology, 120*, 155–159. https://doi.org/10.1007/BF00409102

Cao, J., Wang, J., Wang, S., & Xu, X. (2016). Porphyra Species: A Mini-Review of Its Pharmacological and Nutritional Properties. *Journal of Medicinal Food, 19*(2), 111–119. https://doi.org/10.1089/jmf.2015.3426

549 Chaiklahan, R., Chirasuwan, N., & Bunnag, B. (2012). Stability of phycocyanin extracted from
550 Spirulina sp.: Influence of temperature, pH and preservatives. *Process Biochemistry, 47*(4),
551 659–664. https://doi.org/10.1016/j.procbio.2012.01.010
552 Chang, W. R., Jiang, T., Wan, Z. L., Zhang, J. P., Yang, Z. X., & Liang, D. C. (1996). Crystal structure
553 of R-phycoerythrin from *Polysiphonia urceolata* at 2.8 A resolution. *Journal of Molecular*
554 *Biology, 262*(5), 721–731. https://doi.org/10.1006/jmbi.1996.0547
555 Chen, C.-H., Liu, I.-W., MacColl, R., & Berns, D. S. (1983). Differences in structure and stability
556 between normal and deuterated proteins (phycocyanin). *Biopolymers, 22*(4), 1223–1233.
557 https://doi.org/10.1002/bip.360220414
558 Chi, Z., Hong, B., Tan, S., Wu, Y., Li, H., Lu, C. H., & Li, W. (2020). Impact Assessment of heavy
559 metal cations to the characteristics of photosynthetic phycocyanin. *Journal of Hazardous*
560 *Materials*, *391*, 122225. https://doi.org: 10.1016/j.jhazmat.2020.122225
561 Diaz, C. J., Douglas, K. J., Kang, K., Kolarik, A. L., Malinovski, R., Torres-Tiji, Y., Molino, J. V.,
562 Badary, A., & Mayfield, S. P. (2022). Developing algae as a sustainable food source.
563 *Frontiers in Nutrition, 9*, 1029841. https://doi.org: 10.3389/fnut.2022.1029841
564 Dietzek, B., Maksimenka, R., Hermann, G., Kiefer, W., Popp, J., & Schmitt, M. (2004). The excited-
565 state dynamics of phycocyanobilin in dependence on the excitation wavelength.
566 *Chemphyschem, 5*(8), 1171–1177. https://doi.org: 10.1002/cphc.200400056
567 Edwards, M. R., Hauer, C., Stack, R. F., Eisele, L. E., & MacColl, R. (1997). Thermophilic C-
568 phycocyanin: effect of temperature, monomer stability, and structure. *Biochimica et*
569 *Biophysica Acta, 1321*, 157–164. https://10.1016/S0005-2728(97)00056-X
570 Faieta, M., Neri, L., Sacchetti, G., Di Michele, A., & Pittia, P. (2020). Role of saccharides on thermal
571 stability of phycocyanin in aqueous solutions. *Food Research International, 132*, 109093.
572 https://doi.org: 10.1016/j.foodres.2020.109093
573 Fernandes, R., Campos, J., Serra, M., Fidalgo, J., Almeida, H., Casas, A., Toubarro, D., & Barros, A.
574 (2023). Exploring the Benefits of Phycocyanin: From Spirulina Cultivation to Its Widespread
575 Applications. *Pharmaceuticals (Basel)*, 16(4), 592. https://doi.org: 10.3390/ph16040592.
576 Glazer, A. N., & Hixson, C. S. (1975). Characterisation of R-phycocyanin. Chromophore content of
577 R-phycocyanin and C-phycoerythrin. *Journal of Biological Chemistry, 250*(14), 5487–5495.
578 https://doi.org/10.1016/S0021-9258(19)41208-8
579 Grabowski, J., & Gantt, E. (1978). Photophysical properties of phycobiliproteins from
580 phycobilisomes: fluorescence lifetimes, quantum yields, and polarisation spectra.
581 *Photochemistry and photobiology, 28*(1), 39–45. https://doi.org/10.1111/j.1751-
582 1097.1978.tb06927.x

583 Guo, W., Zeng, M., Zhu, S., Li, S., Qian, Y., & Wu, H. (2022). Phycocyanin ameliorates mouse
584 colitis via phycocyanobilin-dependent antioxidant and anti-inflammatory protection of the
585 intestinal epithelial barrier. *Food & Function, 13*(6), 3294–3307.
586 https://doi.org/10.1039/d1fo02970c
587 Jiang, T., Zhang, J. P., Chang, W. R., & Liang, D. C. (2001). Crystal structure of R-phycocyanin and
588 possible energy transfer pathways in the phycobilisome. *Biophysical Journal, 81*(2), 1171–
589 1179. https://doi.org/10.1016/S0006-3495(01)75774-8
590 Li, W., Pu, Y., Tang, Z., Zhao, F., Xie, M., & Qin, S. (2020). Energy transfer dynamics in B-
591 phycoerythrin from the red alga Porphyridium purpureum. *Chinese Journal of Physics, 66*,
592 24–35. https://doi.org/10.1016/j.cjph.2020.03.025
593 Li, Y., Gillilan, R., & Abbaspourrad, A. (2021). Tuning C-Phycocyanin Photoactivity via pH-
594 Mediated Assembly-Disassembly. *Biomacromolecules, 22*(12), 5128–5138.
595 https://doi.org/10.1021/acs.biomac.1c01095
596 Liu, J. Y., Zhang, J. P., Wan, Z. L., Liang, D. C., Zhang, J. P., & Wu, H. J. (1998). Crystallisation
597 and preliminary X-ray studies of allophycocyanin from red alga Porphyra yezoensis. *Acta*
598 *Crystallographica Section D: Structural Biology, 54*(4), 662–664.
599 https://doi.org/10.1107/s0907444997017824
600 Maghraby, Y. R., El-Shabasy, R. M., Ibrahim, A. H., & Azzazy, H. M. E. (2023). Enzyme
601 Immobilization Technologies and Industrial Applications. *ACS Omega, 8*(6), 5184–5196.
602 https://doi.org/10.1021/acsomega.2c07560
603 McClements, D.J. (2018). Encapsulation, Protection, and Delivery of Bioactive Proteins and Peptides
604 Using Nanoparticle and Microparticle Systems: A Review. *Advances in Colloid and Interface*
605 *Science*, *253*, 1–22. https://doi.org/10.1016/j.cis.2018.02.002
606 Minic, S., Stanic-Vucinic, D., Radomirovic, M., Radibratovic, M., Milcic, M., Nikolic, M., &
607 Cirkovic Velickovic, T. (2018). Characterisation and effects of binding of food-derived
608 bioactive phycocyanobilin to bovine serum albumin. *Food Chemistry, 239*, 1090–1099.
609 https://doi.org/10.1016/j.foodchem.2017.07.066
610 Minic, S. L., Stanic-Vucinic, D., Mihailovic, J., Krstic, M., Nikolic, M. R., & Cirkovic Velickovic,
611 T. (2016). Digestion by pepsin releases biologically active chromopeptides from C-
612 phycocyanin, a blue-colored biliprotein of microalga Spirulina. *Journal of Proteomics, 147*,
613 132–139. https://doi.org: 10.1016/j.jprot.2016.03.043
614 Munier, M., Jubeau, S., Wijaya, A., Morancais, M., Dumay, J., Marchal, L., Jaouen, P., & Fleurence,
615 J. (2014). Physicochemical factors affecting the stability of two pigments: R-phycoerythrin
616 of Grateloupia turuturu and B-phycoerythrin of Porphyridium cruentum. *Food Chemistry,*
617 *150*, 400–407. https://doi.org/10.1016/j.foodchem.2013.10.113

Nikolic, M. R., Minic, S., Macvanin, M., Stanic-Vucinic, D., & Velickovic, T. C. (2020). Analytical Protocols in Phycobiliproteins Analysis. In Jacob-Lopes, M. I. Queiroz & L. Q. Zepka (Eds.), *Pigments from Microalgae*, (pp. 179–201). Springer

Onwezen, M. C., Bouwman, E. P., Reinders, M. J., & Dagevos, H. (2021). A systematic review on consumer acceptance of alternative proteins: Pulses, algae, insects, plant-based meat alternatives, and cultured meat. *Appetite, 159*, 105058. https://doi.org/10.1016/j.appet.2020.105058

Ou, B., Hampsch-Woodill, M., & Prior, R. L. (2001). Development and validation of an improved oxygen radical absorbance capacity assay using fluorescein as the fluorescent probe. *Journal of Agricultural and Food Chemistry, 49*(10), 4619–4626. https://doi.org/10.1021/jf010586o

Pescitelli, G., Gabriel, S., Wang, Y., Fleischhauer, J., Woody, R. W., & Berova, N. (2003). Theoretical analysis of the porphyrin-porphyrin exciton interaction in circular dichroism spectra of dimeric tetraarylporphyrins. *Journal of the American Chemical Society, 125*(25), 7613–7628. https://doi.org/10.1021/ja030047v

Qiao, B. W., Liu, X. T., Wang, C. X., Song, S., Ai, C. Q., & Fu, Y. H. (2022). Preparation, Characterisation, and Antioxidant Properties of Phycocyanin Complexes Based on Sodium Alginate and Lysozyme. *Frontiers in Nutrition, 9*, 890942. https://doi.org/10.3389/fnut.2022.890942

Ramdhan, T., Ching, S. H., Prakash, S., & Bhandari, B. (2020) Physical and mechanical properties of alginate based composite gels. *Trends in Food Science & Technology*, *106*, 150–159. https://doi.org/10.1016/j.tifs.2020.10.002

Rashed, S. A., Hammad, S. F., Eldakak, M. M., Khalil, I. A., & Osman, A. (2023). Assessment of the Anticancer Potentials of the Free and Metal-Organic Framework (UiO-66) - Delivered Phycocyanobilin. *Journal of Pharmaceutical Sciences, 112*(1), 213–224. https://doi.org/10.1016/j.xphs.2022.08.038

Rawiwan, P., Peng, Y., Paramayuda, I. G. P. B., & Quek, S. Y. (2022). Red seaweed: A promising alternative protein source for global food sustainability. *Trends in Food Science & Technology, 123*, 37–56. https://doi.org/10.1016/j.tifs.2022.03.003

Reddy, A., Norris, D. F., Momeni, S. S., Waldo, B., & Ruby, J. D. (2016). The pH of beverages in the United States. *The Journal of the American Dental Association, 147*(4), 255–263. https://doi.org/10.1016/j.adaj.2015.10.019

Saluri, M., Kaldmäe, M., & Tuvikene, R. (2019). Extraction and quantification of phycobiliproteins from the red alga Furcellaria lumbricalis. *Algal Research, 37*, 115–123. https://doi.org/10.1016/j.algal.2018.11.013

Saraswat, S., Desireddy, A., Zheng, D., Guo, L., Lu, H. P., Bigioni, T. P., & Isailovic, D. (2011). Energy Transfer from Fluorescent Proteins to Metal Nanoparticles. *The Journal of Physical Chemistry C, 115*(35), 17587–17593. https://doi.org/10.1021/jp2029246

Saxena, A. M. (1988). Phycocyanin aggregation. A small angle neutron scattering and size exclusion chromatographic study. *Journal of Molecular Biology, 200*(3), 579–591. https://doi.org/10.1016/0022-2836(88)90544-x

Segale, L., Giovannelli, L., Mannina, P., & Pattarino, F. (2016). Calcium Alginate and Calcium Alginate-Chitosan Beads Containing Celecoxib Solubilized in a Self-Emulsifying Phase. *Scientifica (Cairo), 2016*, 5062706. https://doi.org/10.1155/2016/5062706

Simovic, A., Combet, S., Cirkovic Velickovic, T., Nikolic, M., & Minic, S. (2022). Probing the stability of the food colourant R-phycoerythrin from dried Nori flakes. *Food Chemistry, 374*, 131780. https://doi.org/10.1016/j.foodchem.2021.131780

Thureau, A., Roblin, P., & Pérez, J. (2021). BioSAXS on the SWING beamline at Synchrotron SOLEIL. *Journal of Applied Crystallography, 54*(6), 1698–1710. https://doi.org/10.1107/s1600576721008736

Venkatraman, K. L., & Mehta, A. (2019). Health Benefits and Pharmacological Effects of Porphyra Species. *Plant Foods for Human Nutrition, 74*(1), 10–17. https://doi.org/10.1007/s11130-018-0707-9

Wang, L., Qu, Y., Fu, X., Zhao, M., Wang, S., & Sun, L. (2014). Isolation, purification and properties of an R-phycocyanin from the phycobilisomes of a marine red macroalga Polysiphonia urceolata. *PLoS One, 9*(7), e101724. https://doi.org/10.1371/journal.pone.0101724

Yan, S.-G., Zhu, L.-P., Su, H.-N., Zhang, X.-Y., Chen, X.-L., Zhou, B.-C., & Zhang, Y.-Z. (2010). Single-step chromatography for simultaneous purification of C-phycocyanin and allophycocyanin with high purity and recovery from Spirulina (Arthrospira) platensis. *Journal of Applied Phycology, 23*(1), 1–6. https://doi.org/10.1007/s10811-010-9525-7

Zhang, Z., Cho, S. E., Dadmohammadi, Y., Li, Y., & Abbaspourrad, A. (2021). Improvement of the storage stability of C-phycocyanin in beverages by high-pressure processing. *Food Hydrocolloids*, *110*, 106055. https://doi.org/10.1016/j.foodhyd.2020.106055

Zhang, Z., Zhang, R., Zou, L., & McClements, D. J. (2016). Protein encapsulation in alginate hydrogel beads: Effect of pH on microgel stability, protein retention and protein release. *Food Hydrocolloids, 58*, 308–315. https://doi.org/10.1016/j.foodhyd.2016.03.015

Zittelli, G. C., Lauceri, R., Faraloni, C., Benavides, A. M. S., & Torzillo, G. (2023). Valuable pigments from microalgae: phycobiliproteins, primary carotenoids, and fucoxanthin. *Photochemical & Photobiological Sciences*. https://doi.org: 10.1007/s43630-023-00407-3.